Active Fault Tolerant Control based on Backstepping Controller and Non Linear Adaptive Observer for Double Star Induction Machine

Badreddine Ladjal[1, 3]   Fouad Berrabah[3]   Samir Zeghlache[2,3]*   Ali Djerioui[1]
Mohamed Fouad Benkhoris[4]

[1,4]LGE, Laboratory of Electrical Engineering,University of M'sila, Algeria
[2]LASS, Laboratory of Analysis of Signals and Systems, University of M'sila, Algeria
[3]Department of Electrical Engineering, Faculty of Technology, University of M'sila, Algeria
[4]IREENA Laboratory, University of Nantes, Saint-Nazaire, France
* Corresponding author's Email: samir.zeghlache@univ-msila.dz

Abstract: This paper presents an active fault tolerant control (FTC) strategy based on the estimated fault information for a double star induction machine (DSIM) to compensate for faults effects and thus improve the reliability and availability of the machine. The DSIM is powered by two three-phase voltage source inverters (VSI) using pulse width modulation (PWM). A defective dynamic model of DSIM in the rotating synchronous d-q frame with a field-oriented control strategy is developed. The proposed FTC design is based on a backstepping control (BSC) using a nonlinear Thau observer with an adaptive fault estimation law. The Thau observer is used for fault detection and fault reconstruction at the same time. After that, the estimation value of the faults effect is introduced directly into the control law in order to guarantee the stability of the machine in post fault. The sufficient condition for the stability of the closed-loop system (machine + observer) in faulty operation is analyzed and verified using Lyapunov theory. Finally, the efficiency and robustness of the proposed FTC approach are validated in steady state by a numerical simulation developed in MATLAB / Simulink. Obtained results show that the proposed FTC provides a strong fault tolerance where all closed-loop system signals are bounded and errors converge to a small neighborhood of the origin. Simulation results in healthy and faulty conditions confirm the reliability of the suggested framework

Keywords: Double star induction machine, Backstepping control, Fault tolerant control, Nonlinear observer, Stability.

1. Introduction

The double star induction machine (DSIM) belongs to the category of multiphase induction machines (MIM). It has been selected as the best choice because of its many advantages over its three-phase counterpart. The DSIM has been proposed for different fields of industry that need high power such as electric hybrid vehicles, locomotive traction, ship propulsion and many other applications where the safety condintellition is required such as aerospace and offshore wind energy systems. DISM not only guarantees a decrease of rotor harmonics currents and torque pulsations but it also has many other advantages

such as: reliability, power segmentation and higher efficiency. DSIM has a greater fault tolerance; it can continue to operate and maintain rotating flux even with open-phase faults thanks to the greater number of degrees of freedom that it owns compared to the three-phase machines [1]. Nowadays, motors installed in the industry represent 85 % of squirrel cage induction motors because of their many advantages, but because of their continuous use, they are subject to different types of faults: about 40 % to 50 % are bearing faults, 5 % to 10 % are severe rotor faults and 30% to 40% are stator-related faults [2].

Bearing fault (BF) is a defect in different parts of the bearing, such as the inner-raceway, the outer-raceway, the rolling elements and the cage, the
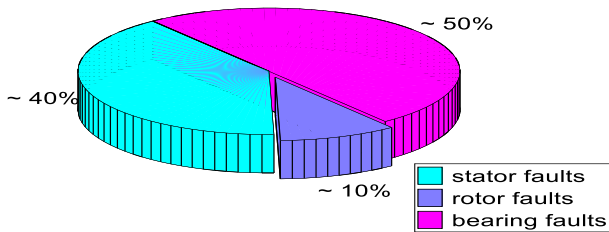
Figure. 1 Faults reparation for classical induction motor

occurrence of the BF is due to impurities inside of the bearing, loss of lubrication or wrong installation [3]. Broken rotor bar (BRB) fault can be caused by failures in the rotor fabrication process, overloads (mechanical stress), mechanical cracks or thermal stress [4]. The most common fault in the stator windings is the inter-turn short-circuits (ITSC). Usually, ITSC faults are caused by insulation failures, mechanical stress, moisture and partial discharge [5]. The occurrence of the faults mentioned above can cause serious damage to DSIM and related equipment and can certainly lead to a sudden shutdown of industrial processes causing significant economic losses. For this reason, there is a major benefit to developing faults tolerant control that compensates the fault effect. The FTC schemes enable a machine to continue operating with an acceptable performance even in the presence of faults, over the past decades, researchers have classified FTC approaches into two types: passive fault-tolerant control (PFTC) and active fault-tolerant control (AFTC). PFTC uses robust control techniques to ensure system insensitivity to closed loop faults. It can maintain the stability of the system when the fault occurs. With PFTC, the system continues to operate with the same controller and system structure, usually; this technique is used in the case where the diagnosis of the fault is difficult to obtain. The PFTC does not require any fault detection and diagnosis system or controller reconfiguration. AFTC is based on online fault compensation and requires online fault information, therefore, this approach needs reconfiguration based on the information provided by the fault detection and identification (FDI) block [6].

FDI in any active fault tolerance strategy is an important area of research nowadays. [7] proposes a fault-tolerance control scheme for DTC of induction motor (IM) drive against the current sensor failures, the sensor fault is identified by a third-difference operator (TDO) and the current corresponding to the faulty phase is estimated by a flux-linkage observer, after the failure, a decision-making logic circuit automatically selects the correct current signal to ensure continuity of operation of the drives. [8] introduces new schemes for detection, isolation, and

compensation of speed and current sensor faults in field oriented IM drives; the novelty in these approaches is that they do not use any type of machine model and motor parameters. [9] Presents an improved sliding mode based faults detection, reconstruction and fault-tolerant control scheme for motor systems with typical actuator faults, a standard sliding mode observer is used to detect and reconstruct the unknown faults presented in the motor model, this combination guarantees tolerance to a wide class of total additive failures. This paper presents a fault tolerant control scheme based on the Thau observer for backstepping control of a double star induction machine. The three main steps involved in the proposed FTC design are fault detection, fault estimation and, finally, fault compensation. Compared to recent work reported in the literature, the contributions of this paper are presented under different aspects such as: fault modeling, control strategy, type of machine processed and type of fault:

- The fault modeling method is based on the motor current signal analysis (MCSA) method, which avoids the use of additional hardware.
- This work consists in proposing a new control strategy to improve the dynamic performance of the double star induction machine, especially in case of faulty operation.
- The combination of the backstepping control and the Thau's observer to design a fault tolerant control scheme for DSIM in presence of the faults.
- Compared to [7, 8], the Thau's robust observer is used for on-line fault estimation and compensation, eliminating the need for a fault detection and isolation module.
- Compared to the work done in [9, 10], the application of the proposed FTC on a DSIM is more advantageous because nowadays the multiphase induction machine is more used than the traditional induction motor in several important areas of the industry.
- Compared to [1, 11], the degree of severity of the fault dealt with in this paper is more important since open phase fault tolerance is a specific feature of multiphase machines thanks to the high number of phases that belong to it.
- Unlike the passive FTC presented in [12], the proposed control structure is not bounded and can simultaneously compensate for three different faults without information of their upper bounds, such as: broken rotor bar fault, stator fault and bearing fault.
- As stated in [13] "A Recent approach for dealing with uncertainties is based on the use of sliding

589

mode method to enhance the robustness of FTCs. However, the problem of FTC design on SMC schemes is still in its early stage of development, and a few results have been reported in the literature". In this contest and considering the existing results, the systemic design of the FTC scheme in this paper focuses on very simple structure, more sensitive detection and a quicker compensation procedure.

This paper is organized as follows: In section 2, the dynamic model of DSIM in healthy condition is given. In section 3, a defective model of the DSIM is presented. An adaptive Thau observer for faults estimation is introduced in section 4. The proposed FTC design is carried out in section 5. Simulation results are presented and analyzed in section 6. Performance comparison in section 7. Finally, the conclusion is given in section 8.

2. DSIM healthy model

DSIM has two stators shifted by an electrical angle and mobile squirrel cage rotor. Each star is composed by three immovable windings which are uniformly distributed and have axes that are shifted from each other an electrical angle equal to $(2\pi/3)$. The Fig. 2 shows an explicit schematic of the stator and rotor windings, α is the angle shift between the two stators and θ is the angle between rotor and stator1 [1]. Usually, the shift angle between the two stators α is equal to 30°.

In order to establish the mathematical model of DSIM, the following assumptions are made:

- Air-gap uniform.
- Magnetic linearity.
- Negligible saturation.
- Stators are identical.

According to the simplifying hypotheses mentioned above, the dynamic healthy model of
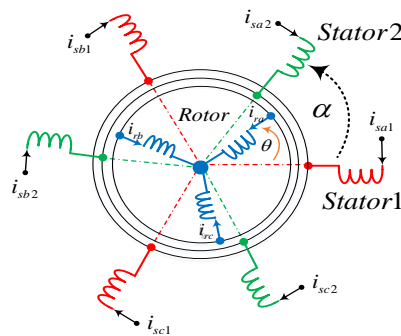

Figure. 2 The DSIM windings

Table 1. Symbols and notations

Symbol	Notation
α	Angle between the stators
ϑ	Angle between rotor and stator1
v_{sd1}, v_{sq1}	Stator1 voltages components
v_{sd2}, v_{sq2}	Stator2 voltages components
i_{sd1}, i_{sq1}	Stator1 currents components
x	Measurable state vector
u	Control input
y	Output state vector
a_i, b_i	Expressed according to the machine parameters
i_{sd2}, i_{sq2}	Stator2 currents components
φ_{rd}, φ_{rq}	Rotor flux components
L_{s1}, L_{s2}, L_r, L_m	Stator1, stator2, rotor and mutual inductance, respectively
R_{s1}, R_{s2}, R_r	Stator1, stator2 and rotor resistance
T_r	Rotor time constant
T_L	Applied load torque
ω_r	Actual rotor speed
J, K_f	Rotor inertia and friction coefficient
ω_s	Stator pulsation
ω_{gl}	Slip pulsation
φ_r	Rotor flux
p	Denotes the number of pole pairs
d, q	Quadrate indices
n_f	Number of all harmonics generated by the faults
f_i	Fault frequency
S	Dynamic matrix
$\hat{f}$	Observer faults vector
Γ	Symmetric matrix
K_{isd1}, K_{isq1}, K_{isd2}, K_{isq2}	Positive gains
$\hat{V}_{sd1}^F, \hat{V}_{sq1}^F$, $\hat{V}_{sd2}^F, \hat{V}_{sq2}^F$	Estimated faults
v_{sd1}^N, v_{sq1}^N, v_{sd2}^N, v_{sq2}^N	Nominal controls designed for healthy functioning
v_{sd1}^{ad}, v_{sq1}^{ad}, v_{sd2}^{ad}, v_{sq2}^{ad}	additive controls

squirrel cage double star induction machine in the d-q axis with a reference frame fixed to the rotor is given by the following system of equation:

$$\begin{cases} \dot{x} = Ax + Bu \\ y = Cx \end{cases} \tag{1}$$

Where: $x = \begin{bmatrix} i_{sd1} & i_{sd2} & i_{sq1} & i_{sq2} & \varphi_r \end{bmatrix}^T$ is the measurable state vector, $u = \begin{bmatrix} v_{sd1} & v_{sd2} & v_{sq1} & v_{sq2} \end{bmatrix}^T$ is the control input, $y = \begin{bmatrix} i_{sd1} & i_{sd2} & i_{sq1} & i_{sq2} \end{bmatrix}^T$ is the output state vector and:

$$\varphi_r = \sqrt{\varphi_{rd}^2 + \varphi_{rq}^2}.$$

$$B = \begin{bmatrix} b_1 & b_2 & 0 & 0 \\ b_2 & b_1 & 0 & 0 \\ 0 & 0 & b_1 & b_2 \\ 0 & 0 & b_2 & b_1 \end{bmatrix},$$

$$A = \begin{bmatrix} a_1 & a_3 & a_2 & 0 & a_4 \\ a_3 & a_1 & 0 & a_2 & a_4 \\ -a_2 & 0 & a_1 & a_3 & -a_5\omega_r \\ 0 & -a_2 & a_3 & a_1 & -a_5\omega_r \\ a_6 & a_6 & 0 & 0 & a_7 \end{bmatrix}$$

,

$$C = \begin{bmatrix} 1 & 0 & 0 & 0 & 0 \\ 0 & 1 & 0 & 0 & 0 \\ 0 & 0 & 1 & 0 & 0 \\ 0 & 0 & 0 & 1 & 0 \end{bmatrix}$$

The mechanical equation is expressed by:

$$\frac{d}{dt}\omega_r = a_8(i_{sq1} + i_{sq2})\varphi_r + a_9\omega_r + a_{10} \qquad (2)$$

The components a_i $i = 1,\overline{1}1$ and b_i $i = 1,\overline{2}$ are expressed according to the machine parameters as follows:

$$a_1 = \frac{R_r L^3{}_m L_r - (R_s(L_m + L_r)^2 + R_r L^2{}_m)(L_m L_s + L_s L_r + L_m L_r)}{(L_m + L_r)[(L_m L_s + L_s L_r + L_m L_r)^2 - L^2{}_m L^2{}_r]}$$

$$a_2 = \omega_s ,$$

$$a_3 = \frac{L_m L_r(R_s(L_m + L_r)^2 + R_r L^2{}_m) - R_r L^2{}_m(L_m L_s + L_s L_r + L_m L_r)}{(L_m + L_r)[(L_m L_s + L_s L_r + L_r L_m)^2 - L^2{}_m L^2{}_r]}$$

$$a_4 = \frac{R_r L_m(L_m L_s + L_s L_r + L_m L_r) - R_r L^2{}_m L_r}{(L_m + L_r)[(L_m L_s + L_s L_r + L_m L_r)^2 - L^2{}_m L^2{}_r]},$$

$$a_5 = \frac{L_m(L_m L_s + L_s L_r + L_m L_r) - L^2{}_m L_r}{(L_m L_s + L_s L_r + L_m L_r)^2 - L^2{}_m L^2{}_r}, \quad a_6 = \frac{L_m R_r}{L_m + L_r} \quad ,$$

$$a_7 = \frac{-R_r}{L_m + L_r}, a_8 = \frac{pL_m}{J(L_m + L_r)}, a_9 = -\frac{K_f}{J},$$

$$a_{10} = -\frac{T_L}{J}, \quad b_1 = \frac{(L_m + L_r)(L_m L_s + L_s L_r + L_m L_r)}{(L_m L_s + L_s L_r + L_m L_r)^2 - L^2{}_m L^2{}_r} \quad ,$$

$$b_2 = -\frac{L_m L_r(L_m + L_r)}{(L_m L_s + L_s L_r + L_m L_r)^2 - L^2{}_m L^2{}_r}$$

Where: v_{sd1}, v_{sq1} are   stator1   voltages components. v_{sd2}, v_{sq2} are   stator2   voltages components. i_{sd1}, i_{sq1} are stator1   currents components.

i_{sd2}, i_{sq2} are   stator2   currents   components. φ_{rd}, φ_{rq} are   rotor   flux   components. L_{s1}, L_{s2}, L_r and L_m are stator1, stator2, rotor and mutual inductance, respectively. R_{s1}, R_{s2} and R_r are respectively stator1, stator2 and rotor resistance. $T_r = L_r/R_r$ is the rotor time constant. T_L is the applied load torque. ω_r is the actual rotor speed. J, K_f denote the rotor inertia and friction coefficient. ω_s is the stator pulsation. ω_{gl} is the slip pulsation. φ_r is the rotor flux. p denotes the number of pole pairs.

Table 2. Frequency related to the fault [14]

Type of faults	Frequency (Hz)
Bearing fault	$f_{bearing} = (f_s + k f_f)$
Stator fault	$f_{stator} = f_s(m(1 - s)/p \pm k)$
BRB fault	$f_{broken} = (1 + 2ks)f_s$

The subscripts d, q designate direct and quadrate indices according to the usual (d-q) axis components in the synchronous rotating frame.

3. DSIM faulty model

In this section, a DSIM model is established in the presence of faults that may be both mechanical and electrical nature due to rotor, stator and bearing failures. According to the researches of [9], the presence of these faults causes an asymmetry of the DSIM and produces harmonic components on the stator currents, so that the two quadratic and direct components of stator current are increased by a sinusoidal component of pulsation $\omega_i = 2\pi f_i$ as follows:

$$\begin{cases} i_{sd} \rightarrow i_{sd} + \sum_i^{n_f} A_i \sin(\omega_i t + \phi_i) \\ i_{sq} \rightarrow i_{sq} + \sum_i^{n_f} A_i \cos(\omega_i t + \phi_i) \\ \quad i = 1, \dots, n_f \end{cases} \qquad (3)$$

Where:

n_f is the number of all harmonics generated by the faults. The amplitude A_i and the phase ϕ_i are unknown parameters; they depend on the fault severity and describe its initial state. f_i represents the fault frequency, its value is known and varies according to the faults type (see Table 2).

Where:

f_f is the frequency that characterizes the vibration, f_s is the supply frequency, $m = 1,2,3,\dots, k = 0,1,3,5,\dots, p$ is the number of pole pairs and s is the per unit slip which given by:

$$s = \frac{synchronous\ speed - rotation speed}{synchronous\ speed} \qquad (4)$$

In order to avoid the uncertainty of the amplitude and phase of the additive harmonics, the sinusoidal generated by the faults can be represented by the following state equation (ecosystem):

$$\dot{z} = S \cdot z \qquad (5)$$

S is a dynamic matrix, its elements are the faults frequencies which are the only known parameters describing the faults and are given by:

$$\begin{cases} S = diag(S_i) \\ S_i = \begin{bmatrix} 0 & \omega_i \\ -\omega_i & 0 \end{bmatrix} \\ i = 1,2,\dots,n_f \end{cases} \quad (6)$$

With: $\begin{cases} size(S) = 2n_f \text{ x } 2n_f \\ size(z) = 2n_f \text{ x } 1 \end{cases}$

The solution of the ecosystem presented in Eq. (5) allows us to rewrite Eq. (3) in the following form:

$$\begin{cases} i_{sd} \rightarrow i_{sd} + Q_d Z \\ i_{sd} \rightarrow i_{sd} + Q_q Z \end{cases} \quad (7)$$

With:

$$\begin{cases} Q_d = [1 \quad 0 \quad 1 \quad 0 \quad . \quad . \quad . \quad 1 \quad 0] \\ Q_q = [0 \quad 1 \quad 0 \quad 1 \quad . \quad . \quad . \quad 0 \quad 1] \end{cases} \quad (8)$$

The time derivative of Eq. (7) is obtained by:

$$\begin{cases} \frac{d}{dt} i_{sd} \rightarrow \frac{d}{dt} i_{sd} + Q_d.S.Z \\ \frac{d}{dt} i_{sq} \rightarrow \frac{d}{dt} i_{sq} + Q_q.S.Z \end{cases} \quad (9)$$

After inserting the additive perturbing terms $Q_d Z$ and $Q_d Z$ and their derivatives $Q_d.S.Z$, $Q_q.S.Z$ respectively in Eq. (1), we obtain the defective model of the DSIM in the stationary reference frame:

$$\begin{cases} \frac{d}{dt} i_{sd1} = a_1 i_{sd1} + a_2 i_{sq1} + a_3 i_{sd2} + a_4 \varphi_r + \\ \qquad b_1 v_{sd1} + b_2 v_{sd2} + V_{sd1}^F \\ \frac{d}{dt} i_{sd2} = a_3 i_{sd1} + a_1 i_{sd2} + a_2 i_{sq2} + a_4 \varphi_r + \\ \qquad b_2 v_{sd1} + b_1 v_{sd2} + V_{sd2}^F \\ \frac{d}{dt} i_{sq1} = -a_2 i_{sd1} + a_1 i_{sq1} + a_3 i_{sq2} - a_5 \varphi_r \omega_r + \\ \qquad b_1 v_{sq1} + b_2 v_{sq2} + V_{sq1}^F \\ \frac{d}{dt} i_{sq2} = a_3 i_{sq1} - a_2 i_{sd2} + a_1 i_{sq2} - a_5 \varphi_r \omega_r + \\ \qquad b_2 v_{sq1} + b_1 v_{sq2} + V_{sq2}^F \\ \frac{d}{dt} \varphi_r = a_6 i_{sd1} + a_6 i_{sd2} + a_7 \varphi_r \end{cases} \quad (10)$$

In this case, Eq. (1) becomes:

$$\begin{cases} \dot{x} = Ax + Bu + Ff \\ y = Cx \end{cases} \quad (11)$$

Where: $F = \begin{bmatrix} 1 & 0 & 0 & 0 \\ 0 & 1 & 0 & 0 \\ 0 & 0 & 1 & 0 \\ 0 & 0 & 0 & 1 \\ 0 & 0 & 0 & 0 \end{bmatrix}$ and,

$f = [V_{sd1}^F \; V_{sd2}^F \; V_{sq1}^F \; V_{sq2}^F]^T = \Gamma z.$

With:

$$\Gamma = \begin{bmatrix} (a_1 + a_3)Q_d + a_2 Q_q - Q_d S \\ (a_1 + a_3)Q_d + a_2 Q_q - Q_d S \\ (a_1 + a_3)Q_q - a_2 Q_d - Q_q S \\ (a_1 + a_3)Q_q - a_2 Q_d - Q_q S \end{bmatrix} \quad (12)$$

4. Fault estimation based on an adaptive Thau observer

4.1 Adaptive Thau observer design

The standard observer of Thau which estimates Eq. (1) is given by [15]:

$$\begin{cases} \dot{\hat{x}} = A\hat{x} + Bu + K(y - \hat{y}) \\ \hat{y} = C\hat{x} \end{cases} \quad (13)$$

Where:
$\hat{x} \in \mathbb{R}^5$ is the observer state vector, $\hat{y} \in \mathbb{R}^4$ is the observer output vector, K is the gain of the observer. According to theorem 1 of [16], K satisfies that the state model of Eq. (13) is an asymptotic estimate of the machine model defined by Eq. (1) only if the following equation is valid:

$$K = P_\theta^{-1} C^T \quad (14)$$

Where:
P_θ is a positive definite solution of the following Lyapunov function:

$$A^T P_\theta + P_\theta A - C^T C + \theta C^T P_\theta = 0 \quad (15)$$

With $(\theta > 0)$
In this case, the error e tends to zero when t tends to infinity:

$$\lim_{t\to\infty} e(t) = \lim_{t\to\infty} (x(t) - \hat{x}(t)) = 0 \quad (16)$$

However, in case of faulty operation when $e_y = y - \hat{y} \neq 0$, the standard observer is not able to make a reliable estimate, for this reason and in order to fix the estimation problem when faults occur, an adaptive Thau observer is suggested to detect faults and estimate their parameters at the same time, its strategy is based on fault detection provided by the
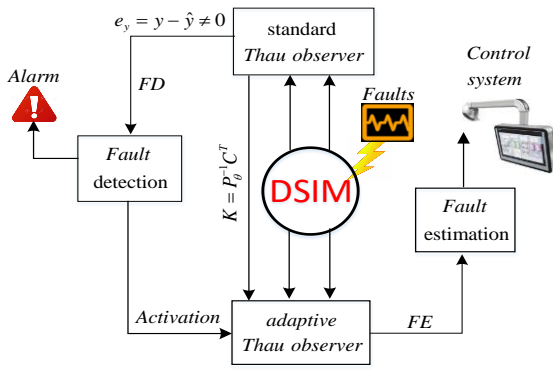
Figure. 3 Fault detection structure for the DSM

standard Thau observer [16]. The fault detection and estimation process is represented in Fig. 3. The new nonlinear observer is given by [15]:

$$\begin{cases} \dot{\hat{x}} = A\hat{x} + Bu + F\hat{f} + K(y - \hat{y}) \\ \hat{y} = C\hat{x} \end{cases} \quad (17)$$

Where:

$\hat{f}$ is the observer faults vector.

4.2 Adaptive Thau observer stability

Assumption :

Let be the following system of equation:

$$\begin{cases} P(A - KC) + (A - KC)^T P + \gamma PP + \gamma I = -Q \\ PB = C^T G^T \end{cases} \quad (18)$$

Where:

γ is a positive parameter, $[Q]_{n \times n} > 0$, the matrixes $[P]_{n \times n}$ and $[G]_{n \times n}$ are a solution of Eq. (18).

Definition:

The dynamics of the estimation error is defined by:

$$\begin{cases} \dot{e}_x = (A - KC)e_x + F\, e_f \\ e_x = x - \hat{x} \end{cases} \quad (19)$$

The estimation error of the faults is indicated by:

$$e_f = f - \hat{f} = \begin{bmatrix} \tilde{V}_{sd1}^F \\ \tilde{V}_{sq1}^F \\ \tilde{V}_{sd2}^F \\ \tilde{V}_{sq2}^F \end{bmatrix} = \begin{bmatrix} V_{sd1}^F - \hat{V}_{sd1}^F \\ V_{sq1}^F - \hat{V}_{sq1}^F \\ V_{sd2}^F - \hat{V}_{sd2}^F \\ V_{sq2}^F - \hat{V}_{sq2}^F \end{bmatrix} \quad (20)$$

The square module of e_f is given by:

$$\| e_f \|^2 =$$
$$\left(\tilde{V}_{sd1}^F \right)^2 + \left(\tilde{V}_{sq1}^F \right)^2 + \left(\tilde{V}_{sd2}^F \right)^2 + \left(\tilde{V}_{sq2}^F \right)^2 \quad (21)$$

The estimation error is presented by:

$$e_x = \begin{bmatrix} i_{sd1} - \hat{\imath}_{sd1} \\ i_{sq1} - \hat{\imath}_{sq1} \\ i_{sd2} - \hat{\imath}_{sd2} \\ i_{sq2} - \hat{\imath}_{sq2} \\ \varphi_r - \hat{\phi}_r \end{bmatrix} \quad (22)$$

The dynamic of the adaptive fault estimation law is defined as follows [16]:

$$\dot{\hat{f}} = \Gamma G(y - \hat{y}) - \sigma\, \Gamma \hat{f} \quad (23)$$

Where Γ is a symmetric matrix that checks:

$$\begin{cases} \Gamma = \Gamma^T \\ \Gamma > 0 \end{cases} \quad (24)$$

Usually, Γ called weighing matrix, its role is to guarantees the convergence of the observer presented by (13). σ is a positive constant that must verify the following inequality:

$$\sigma - \lambda_{\max}(\Gamma^{-1}) > 0 \quad (25)$$

Where: $\lambda_{\max}$ is the maximum eigenvalue of Γ^{-1}.
The following theorem holds.

Theorem:

The observer presented in Eq. (17) that adopts Eq. (23), can guarantee that the following steady-state error limits tend to zero i.e. [16]:

$$\begin{cases} \lim_{x \to \infty} e_x = 0 \\ \lim_{x \to \infty} e_f = 0 \end{cases} \quad (26)$$

Proof:

The time derivative of the estimation error is computed by:

$$\dot{e}_f = \dot{f} - \Gamma G\, e_y + \sigma\, \Gamma f - \sigma\, \Gamma e_f \quad (27)$$

Consider the following Lyapunov function:

$$V_{obs} = e_x^T P\, e_x + e_f^T\, \Gamma^{-1}\, e_f > 0 \quad (28)$$

The time derivative of (28) is given by:

$$\dot{V}_{obs} = e_x^T[(A-KC)^TP + P(A-KC)]e_x + 2e_f^T\Gamma^{-1}\dot{f} + 2\sigma e_f^T f - 2\sigma e_f^T e_f \quad (29)$$

Properties:

According to [16, 17], we can exploit these properties in the rest of the paper:

$$2e_f^T\Gamma^{-1}\dot{f} \leq \lambda_{\max}(\Gamma^{-1})\|e_f\|^2 + \lambda_{\max}(\Gamma^{-1})f_1^2 \quad (30)$$

$$2\sigma e_f^T f \leq \sigma\|e_f\|^2 + \sigma f_0^2 \quad (31)$$

Where:

$$\sigma > 0 \text{ And } \begin{cases} |f| \leq f_0 \\ |\dot{f}| \leq f_1 \end{cases}.$$

$$2\sigma e_f^T e_f = 2\sigma\|e_f\|^2 \quad (32)$$

$$e_x^T Q e_x \leq -\lambda_{\min}(Q)\|e_x\|^2 \quad Q > 0 \quad (33)$$

Where:

$\lambda_{\min}(.)$ is the maximum eigenvalue of Q.

Using the properties mentioned above, we can make the following inequality:

$$\dot{V}_{obs} \leq e_x^T[(A-KC)^TP + P(A-KC) + \gamma PP + \gamma I]e_x + \lambda_{\max}(\Gamma^{-1})[\|e_f^2\| + f_1^2] + \sigma[\|e_f^2\| + f_0^2] - 2\sigma\|e_f\|^2 \quad (34)$$

$$\leq -\lambda_{\min}(Q)\|e_x\|^2 - [\sigma - \lambda_{\max}(\Gamma^{-1})]\|e_f\|^2 + \lambda_{\max}(\Gamma^{-1}).f_1^2 + \sigma f_0^2 \quad (35)$$

Where:

$\lambda_{\min}(.)$ is the minimum eigenvalue of Q and, $\lambda_{\max}(.)$ is the maximum eigenvalue of Γ^{-1}.

Finally, if $\sigma - \lambda_{\max}(\Gamma^{-1}) > 0$, the inequality below holds:

$$\dot{V}_{obs} \leq -c\left[\|e_x\|^2 + \|e_f\|^2\right] < 0 \quad (36)$$

Where:

c is a positive parameter that checks:

$$c = \min[\lambda_{\min}(Q), \sigma - \lambda_{\max}(\Gamma^{-1})] \quad (37)$$

Hence the convergence of estimates errors to zero is proven, which guarantees the stability of the adaptive Thau observer, despite the presence of faults.

5. Control strategy of the DSIM in presence of the faults

In this section, a systematic FTC scheme based on fault estimation is designed to compensate for the faults effect respecting the stability and convergence of the system according to the Lyapunov theory. The currents i_{sd1}, i_{sq1}, i_{sd2} and i_{sq2} and the speed are supposed to be measured. The dynamic equations of DSIM are nonlinear. Using the backstepping strategy, the system is gradually controlled, step by step, from virtual controls (stator currents) to real controls (stator voltages). It is clearly demonstrated in the state equation of the defective DSIM model presented in Eq. (11) that the rotor flux can be controlled by the sum of the components of the stator current i_{sd1} and i_{sd2}. The speed ω_r is adjusted by $i_{sq1} + i_{sq2}$ as shown in Eq. (2). On the other hand, the currents in turn are controlled by the stator voltages v_{sd1}, v_{sq1}, v_{sd2}, and v_{sq2}. Therefore, the design of the proposed FTC is presented by a feedback structure with two consecutive steps.

5.1 Step 1: speed and flux control

This step forces the rotor flux φ_r and the speed ω_r to reach their desired references φ_r^* and ω_r^*, respectively, by identifying their errors Z_φ and Z_ω and that means finding the virtual control that guarantees this convergence. Flux and speed tracking errors are given by:

$$\begin{cases} Z_\omega = \omega_r^* - \omega_r \\ Z_\varphi = \varphi_r^* - \varphi_r \end{cases} \quad (38)$$

The derivation of Eq. (38) gives:

$$\begin{cases} \dot{Z}_\omega = \dot{\omega}_r^* - \dot{\omega}_r \\ \dot{Z}_\varphi = \dot{\varphi}_r^* - \dot{\varphi}_r \end{cases} \quad (39)$$

Using (2) and (10), (39) becomes:

$$\begin{cases} \dot{Z}_\omega = \dot{\omega}_r^* - [a_8(i_{sq1} + i_{sq2})\varphi_r + a_9\omega_r + a_{10}] \\ \dot{Z}_\varphi = \dot{\varphi}_r^* - [a_6(i_{sd1} + i_{sd2}) + a_7\varphi_r] \end{cases} \quad (40)$$

The first Lyapunov candidate function adapted to rotor flux and speed errors is defined by:

$$V_1 = \frac{1}{2}(Z_\varphi^2 + Z_\omega^2) \quad (41)$$

The time derivative of Eq. (41) is obtained by:

$$\dot{V}_1 = Z_\varphi \dot{Z}_\varphi + Z_\omega \dot{Z}_\omega \qquad (42)$$

To achieve stability according to the Lyapunov theory, the derivative of V_1 must be defined negative, in this case, we take:

$$\begin{cases} \dot{Z}_\varphi = -K_\varphi Z_\varphi \\ \dot{Z}_\omega = -K_\omega Z_\omega \end{cases} \qquad (43)$$

Replacing Eq. (43) into Eq. (42), the derivative of the first Lyapunov function becomes:

$$\dot{V}_1 = -K_\varphi Z_\varphi^2 - K_\omega Z_\omega^2 \qquad (44)$$

$\dot{V}_1 < 0$ is always satisfied $\forall K_\varphi, K_\omega > 0$, therefore, the values of Eq. (43) ensure the stability of the closed-loop subsystem. By equating Eq. (40) with Eq. (43), we obtain:

$$\begin{cases} -K_\omega Z_\omega = \dot{\omega}_r^* - [a_8(i_{sq1} + i_{sq2})\varphi_r + a_9\omega_r + a_{10}] \\ -K_\varphi Z_\varphi = \dot{\varphi}_r^* - [a_6(i_{sd1} + i_{sd2}) + a_7\varphi_r] \end{cases} \qquad (45)$$

Posing:

$$\begin{cases} i_{sd1} + i_{sd2} = i_{sd}^* \\ i_{sq1} + i_{sq2} = i_{sq}^* \end{cases} \qquad (46)$$

And assuming that:

$$\begin{cases} i_{sd1}^* = i_{sd2}^* = \dfrac{i_{sd}^*}{2} \\ i_{sq1}^* = i_{sq2}^* = \dfrac{i_{sq}^*}{2} \end{cases} \qquad (47)$$

Finally, the virtual elements of control are given by:

$$\begin{cases} i_{sd}^* = \dfrac{1}{a_6}[\dot{\varphi}_r^* - a_7\varphi_r + K_\varphi Z_\varphi] \\ i_{sq}^* = \dfrac{1}{a_8}[\dot{\omega}_r^* - a_9\omega_r - a_{10} + K_\omega Z_\omega] \end{cases} \qquad (48)$$

5.2 Step 2: currents control

This step establishes the control law by forcing the currents i_{sd1}, i_{sq1}, i_{sd2}, i_{sq2} resulting from the first step to reach their desired references i_{sd1}^*, i_{sq1}^*, i_{sd2}^*, i_{sq2}^* respectively; this objective requires the identification of four new errors. The tracking errors of the currents are:

$$\begin{cases} Z_{isd1} = i_{sd1}^* - i_{sd1} \\ Z_{isq1} = i_{sq1}^* - i_{sq1} \\ Z_{isd2} = i_{sd2}^* - i_{sq2} \\ Z_{isq2} = i_{sq2}^* - i_{sq2} \end{cases} \qquad (49)$$

The derivation of Eq. (49) gives:

$$\begin{cases} \dot{Z}_{isd1} = \dfrac{d}{dt}i_{sd1}^* - \dfrac{d}{dt}i_{sd1} \\ \dot{Z}_{isq1} = \dfrac{d}{dt}i_{sq1}^* - \dfrac{d}{dt}i_{sq1} \\ \dot{Z}_{isd2} = \dfrac{d}{dt}i_{sd2}^* - \dfrac{d}{dt}i_{sd2} \\ \dot{Z}_{isq2} = \dfrac{d}{dt}i_{sq2}^* - \dfrac{d}{dt}i_{sq2} \end{cases} \qquad (50)$$

By substituting the derivatives of the currents from Eq. (10) in Eq. (50), we obtain:

$$\begin{cases} \dot{Z}_{isd1} = \dfrac{d}{dt}i_{sd1}^* - (f_1 + b_1 v_{sd1} + b_2 v_{sd2} + V_{sd1}^F) \\ \dot{Z}_{isq1} = \dfrac{d}{dt}i_{sq1}^* - (f_2 + b_1 v_{sq1} + b_2 v_{sq2} + V_{sq1}^F) \\ \dot{Z}_{isd2} = \dfrac{d}{dt}i_{sd2}^* - (f_3 + b_2 v_{sd1} + b_1 v_{sd2} + V_{sd2}^F) \\ \dot{Z}_{isq2} = \dfrac{d}{dt}i_{sq2}^* - (f_4 + b_2 v_{sq1} + b_1 v_{sq2} + V_{sq2}^F) \end{cases} \qquad (51)$$

With,

$$f = \begin{bmatrix} f_1 \\ f_2 \\ f_3 \\ f_4 \end{bmatrix} = \begin{bmatrix} a_1 i_{sd1} + a_2 i_{sq1} + a_3 i_{sd2} + a_4\varphi_r \\ -a_2 i_{sd1} + a_1 i_{sq1} + a_3 i_{sq2} - a_5\varphi_r\omega_r \\ a_3 i_{sd1} + a_1 i_{sd2} + a_2 i_{sq2} + a_4\varphi_r \\ a_3 i_{sq1} - a_2 i_{sd2} + a_1 i_{sq2} - a_5\varphi_r\omega_r \end{bmatrix} \qquad (52)$$

We note that the actual control variables $v_{sd1}, v_{sq1}, v_{sd2}$ and v_{sq2} have appeared in Eq. (51), so the increased function of Lyapunov V_2 is chosen as follows:

$$V_2 = \frac{1}{2}(Z_\omega^2 + Z_\varphi^2) + V_{currents} + \frac{1}{4m}V_{OBS}, m > 0 \qquad (53)$$

Where:

$$\begin{cases} V_{currents} = \frac{1}{2}Z_{isd1}^2 + \frac{1}{2}Z_{isq1}^2 + \frac{1}{2}Z_{isd2}^2 + \frac{1}{2}Z_{isq2}^2 \\ V_{OBS} = (e_x^T p e_x^T + e_f p^{-1} e_f) \end{cases} \qquad (54)$$

From Eq. (35), we have:

$$\dot{V}_{OBS} \leq -\lambda_{\min}(Q)\|e_x\|^2 - [\sigma - \lambda_{\max}(\Gamma^{-1})]\|e_f\|^2 \qquad (55)$$

Putting:

$$\begin{cases} c_1 = \lambda_{\min}(Q) > 0 \\ c_2 = \sigma - \lambda_{\max}(\Gamma^{-1}) > 0 \end{cases} \quad (56)$$

The inequality (55) becomes:

$$\dot{V}_{OBS} \le -c_1\|e_x\|^2 - c_2\|e_f\|^2 \quad (57)$$

The stability of the observer requires that $\|e_x\| = 0$, in this case we have:

$$\dot{V}_{OBS} \le -c_2\|e_f\|^2 \quad (58)$$

According to (58), the time derivative of V_2 can be written as follows:

$$\dot{V}_2 \le \dot{V}_1 + \left(Z_{isd1}\dot{Z}_{isd1} + Z_{isq1}\dot{Z}_{isq1} + Z_{isd2}\dot{Z}_{isd2} + Z_{isq2}\dot{Z}_{isq2}\right) - \frac{1}{4m}c_2\|e_f\|^2 \quad (59)$$

$$\dot{V}_2 \le \dot{V}_1 + \left(Z_{isd1}\dot{Z}_{isd1} + Z_{isq1}\dot{Z}_{isq1} + Z_{isd2}\dot{Z}_{isd2} + Z_{isq2}\dot{Z}_{isq2}\right) - \frac{1}{4m'}\|e_f\|^2 \quad (60)$$

With: $m' = \frac{m}{c_2}$

Replacing Eq. (21) into Eq. (60), we obtain:

$$\dot{V}_2 \le \dot{V}_1 + Z_{isd1}\dot{Z}_{isd1} + Z_{isq1}\dot{Z}_{isq1} + Z_{isd2}\dot{Z}_{isd2} + Z_{isq2}\dot{Z}_{isq2} - \frac{1}{4m'}\left[\left(\tilde{V}_{sd1}^F\right)^2 + \left(\tilde{V}_{sq1}^F\right)^2 + \left(\tilde{V}_{sd2}^F\right)^2 + \left(\tilde{V}_{sq2}^F\right)^2\right] \quad (61)$$

Using Eq. (51), Eq. (61) becomes:

$$\dot{V}_2 \le \dot{V}_1 + Z_{isd1}\left(\frac{d}{dt}i_{sd1}^* - f_1 - b_1 v_{sd1} - b_2 v_{sd2} - \tilde{V}_{sd1}^F\right) - \frac{1}{4m'}\left(\tilde{V}_{sd1}^F\right)^2 + Z_{isq1}\left(\frac{d}{dt}i_{sq1}^* - f_2 - b_1 v_{sq1} - b_2 v_{sq2} - \tilde{V}_{sq1}^F\right) - \frac{1}{4m'}\left(\tilde{V}_{sq1}^F\right)^2 + Z_{isd2}\left(\frac{d}{dt}i_{sd2}^* - f_3 - b_2 v_{sd1} - b_1 v_{sd2} - V_{sd2}^F\right) - \frac{1}{4m'}\left(\tilde{V}_{sd2}^F\right)^2 + Z_{isq2}\left(\frac{d}{dt}i_{sq2}^* - f_4 - b_2 v_{sq1} - b_1 v_{sq2} - V_{sq2}^F\right) - \frac{1}{4m'}\left(\tilde{V}_{sq2}^F\right)^2 \quad (62)$$

The inequality Eq. (62) can be rewritten in this form:

$$\dot{V}_2 \le \dot{V}_1 + Z_{isd1}\left(\frac{d}{dt}i_{sd1}^* - f_1 - b_1 v_{sd1} - b_2 v_{sd2} - \left(\tilde{V}_{sd1}^F + \hat{V}_{sd1}^F\right)\right) - \frac{1}{4m'}\left(\tilde{V}_{sd1}^F\right)^2 + Z_{isq1}\left(\frac{d}{dt}i_{sq1}^* - \right.$$

$$f_2 - b_1 v_{sq1} - b_2 v_{sq2} - \left(\tilde{V}_{sq1}^F + \hat{V}_{sq1}^F\right)\right) -$$

$$\frac{1}{4m'}\left(\tilde{V}_{sq1}^F\right)^2 +$$

$$Z_{isd2}\left(\frac{d}{dt}i_{sd2}^* - f_3 - b_2 v_{sd1} - b_1 v_{sd2} - \left(\tilde{V}_{sd2}^F + \hat{V}_{sd2}^F\right)\right) - \frac{1}{4m'}\left(\tilde{V}_{sd2}^F\right)^2 +$$

$$Z_{isq2}\left(\frac{d}{dt}i_{sq2}^* - f_4 - b_2 v_{sq1} - b_1 v_{sq2} - \left(\tilde{V}_{sq2}^F + \hat{V}_{sq2}^F\right)\right) - \frac{1}{4m'}\left(\tilde{V}_{sq2}^F\right)^2 \quad (63)$$

By adding and subtracting the terms $m' Z_{isdi}$ $i = \overline{1,4}$ in Eq. (63), we get:

$$\dot{V}_2 \le \dot{V}_1 + Z_{isd1}\left(\frac{d}{dt}i_{sd1}^* - f_1 - b_1 v_{sd1} - b_2 v_{sd2} + m' Z_{isd1} - \hat{V}_{sd1}^F\right) + Z_{isq1}\left(\frac{d}{dt}i_{sq1}^* - f_2 - b_1 v_{sq1} - b_2 v_{sq2} + m' Z_{isq1} - \hat{V}_{sq1}^F\right) + Z_{isd2}\left(\frac{d}{dt}i_{sd2}^* - f_3 - b_2 v_{sd1} - b_1 v_{sd2} + m' Z_{isd2} - \hat{V}_{sd2}^F\right) + Z_{isq2}\left(\frac{d}{dt}i_{sq2}^* - f_4 - b_2 v_{sq1} - b_1 v_{sq2} + m' Z_{isq2} - \hat{V}_{sq2}^F\right) - m'\left[\left(Z_{isd1} + \frac{1}{2m'}\tilde{V}_{sd1}^F\right)^2 + \left(Z_{isq1} + \frac{1}{2m'}\tilde{V}_{sq1}^F\right)^2 + \left(Z_{isd2} + \frac{1}{2m'}\tilde{V}_{sd2}^F\right)^2 + \left(Z_{isq2} + \frac{1}{2m'}\tilde{V}_{sq2}^F\right)^2\right] \quad (64)$$

To have $\dot{V}_2$ definite negative, we do:

$$\begin{cases} \frac{d}{dt}i_{sd1}^* - f_1 - b_1 v_{sd1} - b_2 v_{sd2} + m' Z_{isd1} - \\ \qquad \hat{V}_{sd1}^F = -K_{isd1}Z_{isd1} \\ \frac{d}{dt}i_{sq1}^* - f_2 - b_1 v_{sq1} - b_2 v_{sq2} + m' Z_{isq1} - \\ \qquad \hat{V}_{sq1}^F = -K_{isq1}Z_{isq1} \\ \frac{d}{dt}i_{sd2}^* - f_3 - b_2 v_{sd1} - b_1 v_{sd2} + m' Z_{isd2} - \\ \qquad \hat{V}_{sd2}^F = -K_{isd2}Z_{isd2} \\ \frac{d}{dt}i_{sq2}^* - f_4 - b_2 v_{sq1} - b_1 v_{sq2} + m' Z_{isq2} - \\ \qquad \hat{V}_{sq2}^F = -K_{isq2}Z_{isq2} \end{cases} \quad (65)$$

Where: K_{isd1}, K_{isq1}, K_{isd2} and K_{isq2} are the positive gains that adjust the overall stability of the closed-loop system. Finally, the fault-tolerant control based on a non-linear observer is represented by the following components of the stator voltages:

$$v_{sd1} = \frac{b_1}{b_1^2 - b_2^2}\frac{d}{dt}i_{sd1}^* - \frac{b_2}{b_1^2 - b_2^2}\frac{d}{dt}i_{sd2}^* - \frac{b_1}{b_1^2 - b_2^2}f_1 + \frac{b_2}{b_1^2 - b_2^2}f_3 - \frac{b_1}{b_1^2 - b_2^2}\hat{V}_{sd1}^F + \frac{b_2}{b_1^2 - b_2^2}\hat{V}_{sd2}^F + \frac{b_1}{b_1^2 - b_2^2}(m_1' + K_{isd1})Z_{isd1} - \frac{b_2}{b_1^2 - b_2^2}(m_1' + K_{isd2})Z_{isd2}$$

$$(66)$$

$$v_{sd2} = -\frac{b_2}{b_1^2 - b_2^2}\frac{d}{dt}i_{sd1}^* + \frac{b_1}{b_1^2 - b_2^2}\frac{d}{dt}i_{sd2}^* + \frac{b_2}{b_1^2 - b_2^2}f_1 -$$
$$\frac{b_1}{b_1^2 - b_2^2}f_3 + \frac{b_2}{b_1^2 - b_2^2}\hat{V}_{sd1}^F - \frac{b_1}{b_1^2 - b_2^2}\hat{V}_{sd2}^F - \frac{b_2}{b_1^2 - b_2^2}(m_1' +$$
$$K_{isd1})Z_{isd1} + \frac{b_1}{b_1^2 - b_2^2}(m_1' + K_{isd2})Z_{isd2} \qquad (67)$$

$$v_{sq1} = \frac{b_1}{b_1^2 - b_2^2}\frac{d}{dt}i_{sq1}^* - \frac{b_2}{b_1^2 - b_2^2}\frac{d}{dt}i_{sq2}^* - \frac{b_1}{b_1^2 - b_2^2}f_2 +$$
$$\frac{b_2}{b_1^2 - b_2^2}f_4 - \frac{b_1}{b_1^2 - b_2^2}\hat{V}_{sq1}^F + \frac{b_2}{(b_1^2 - b_2^2)}\hat{V}_{sq2}^F +$$
$$\frac{b_1}{(b_1^2 - b_2^2)}(K_{isq1} + m_1')Z_{isq1} - \frac{b_2}{(b_1^2 - b_2^2)}(K_{isq2} +$$
$$m_1')Z_{isq2} \qquad (68)$$

$$v_{sq2} = -\frac{b_2}{b_1^2 - b_2^2}\frac{d}{dt}i_{sq1}^* + \frac{b_1}{b_1^2 - b_2^2}\frac{d}{dt}i_{sq2}^* + \frac{b_2}{b_1^2 - b_2^2}f_2 -$$
$$\frac{b_1}{b_1^2 - b_2^2}f_4 + \frac{b_2}{b_1^2 - b_2^2}\hat{V}_{sq1}^F - \frac{b_1}{b_1^2 - b_2^2}\hat{V}_{sq2}^F -$$
$$\frac{b_2}{b_1^2 - b_2^2}(m_1' + K_{isq1})Z_{isq1} + \frac{b_1}{b_1^2 - b_2^2}(m_1' + K_{isq2})Z_{isq2}$$
$$(69)$$

The control law presented by Eq. (66) – Eq. (69) can be formulated like follow:

$$\begin{bmatrix} v_{sd1} \\ v_{sd2} \\ v_{sq1} \\ v_{sq2} \end{bmatrix} = \begin{bmatrix} v_{sd1}^N \\ v_{sd2}^N \\ v_{sq1}^N \\ v_{sq2}^N \end{bmatrix} + \begin{bmatrix} v_{sd1}^{ad} \\ v_{sd2}^{ad} \\ v_{sq1}^{ad} \\ v_{sq2}^{ad} \end{bmatrix} \qquad (70)$$

Where: v_{sd1}^N, v_{sq1}^N, v_{sd2}^N and v_{sq2}^N are the backstepping control laws called the nominal controls designed for healthy functioning (when $f = [V_{sd1}^F \ V_{sd2}^F \ V_{sq1}^F \ V_{sq2}^F]^T = [0]^T$), their role is to correctly manage flux and speed tracking by compensating for the load disturbance:

$$\begin{cases} v_{sd1}^N = \frac{1}{b_1^2 - b_2^2}(b_1\frac{d}{dt}i_{sd1}^* - b_2\frac{d}{dt}i_{sd2}^* - \\ b_1f_1 + b_2f_3 + b_1G_{isd1}Z_{isd1} - b_2G_{isd2}Z_{isd2}) \\ v_{sd2}^N = \frac{1}{b_1^2 - b_2^2}(-b_2\frac{d}{dt}i_{sd1}^* + b_1\frac{d}{dt}i_{sd2}^* + \\ b_2f_1 - b_1f_3 + b_2G_{isd1}Z_{isd1} + b_1G_{isd2}Z_{isd2}) \end{cases}$$

And,

$$\begin{cases} v_{sq1}^N = \frac{1}{b_1^2 - b_2^2}(b_1\frac{d}{dt}i_{sq1}^* - b_2\frac{d}{dt}i_{sq2}^* - \\ b_1f_2 + b_2f_4 + b_1G_{isq1}Z_{isq1} - b_2G_{isq2}Z_{isq2}) \\ v_{sq2}^N = \frac{1}{b_1^2 - b_2^2}(-b_2\frac{d}{dt}i_{sq1}^* + b_1\frac{d}{dt}i_{sq2}^* + \\ b_2f_2 - b_1f_4 + b_2G_{isq1}Z_{isq1} + b_1G_{isq2}Z_{isq2}) \end{cases} \qquad (70)$$
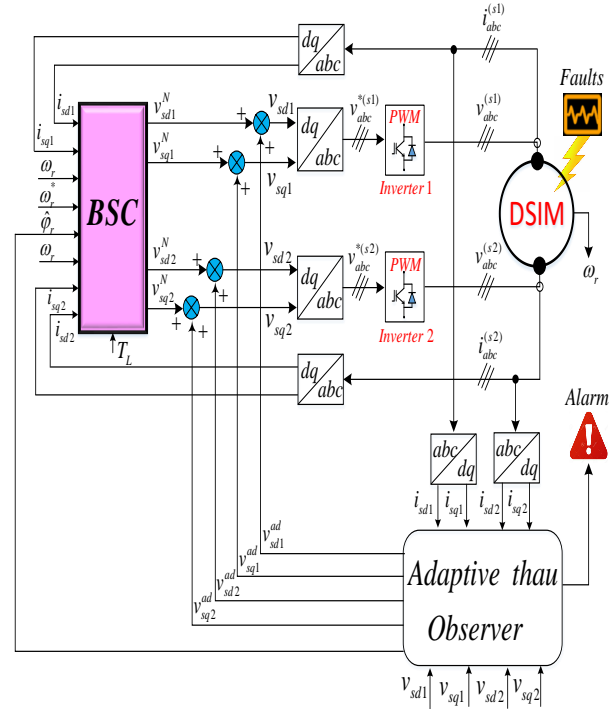

Figure. 4 Block diagram of the global AFTC for DSIM

With:

$$\begin{cases} G_{isd1} = K_{isd1} + m' > 0 \\ G_{isd2} = K_{isd2} + m' > 0 \\ G_{isq1} = K_{isq1} + m' > 0 \\ G_{isq2} = K_{isq2} + m' > 0 \end{cases} \qquad (72)$$

And, v_{sd1}^{ad}, v_{sq1}^{ad}, v_{sd2}^{ad}, v_{sq2}^{ad} are additive controls, their role is to reconfigure the nominal controls to compensate for faults. In the absence of faults, we have: $v_{sd1}^{ad} = v_{sq1}^{ad} = v_{sd2}^{ad} = v_{sq2}^{ad} = 0$. These compensation units are expressed by:

$$\begin{bmatrix} v_{sd1}^{ad} \\ v_{sd2}^{ad} \\ v_{sq1}^{ad} \\ v_{sq2}^{ad} \end{bmatrix} = \begin{bmatrix} -\begin{bmatrix} b_1 & b_2 \\ b_2 & b_1 \end{bmatrix}^{-1} & [0]_{2x2} \\ [0]_{2x2} & -\begin{bmatrix} b_1 & b_2 \\ b_2 & b_1 \end{bmatrix}^{-1} \end{bmatrix} \begin{bmatrix} \hat{V}_{sd1}^F \\ \hat{V}_{sd2}^F \\ \hat{V}_{sq1}^F \\ \hat{V}_{sq2}^F \end{bmatrix} \qquad (73)$$

Where: $\hat{V}_{sd1}^F$, $\hat{V}_{sq1}^F$, $\hat{V}_{sd2}^F$, and $\hat{V}_{sq2}^F$ are the estimated faults given by the adaptive observer of Thau. The global block diagram of the proposed FTC is shown in Fig. 4. In order to protect the machine and associated equipment against damage and thus prevent the sudden stop of industrial processes that can cause significant economic loss, an alarm indicator is added to the design. The alarm signal indicates that maintenance is needed.
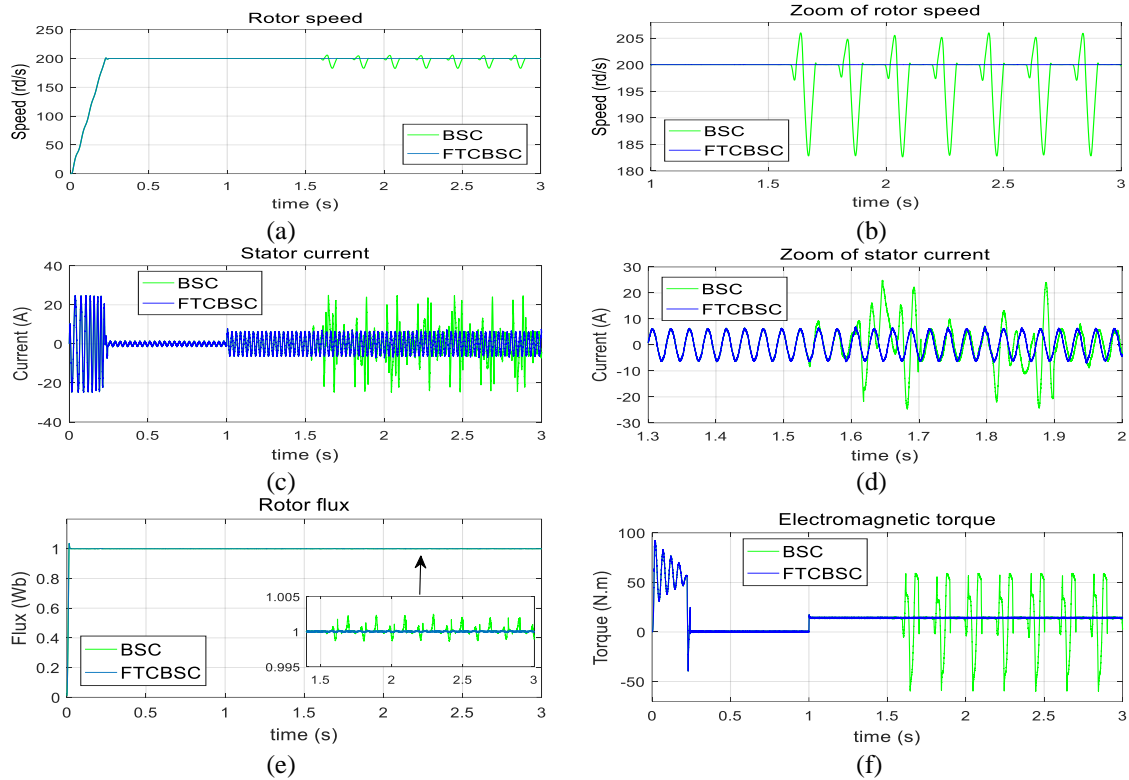
Figure. 5 Simulation results in case of three faults (BF, ITSC and BRB) affect the DSIM at time t=1.5 s using BSC and the proposed FTC: (a) rotor speed, (b) zoom of rotor speed, (c) stator current, (d) zoom of stator current, (e) rotor flux, and (f) electromagnetic torque

Table 3. Machine parameters [1]

Parameters	Identifiers & values
Voltage	230-380 V
frequency	50 Hz
Stator resistance	$R_{s1} = R_{s2} = 3.72\ \Omega$
Rotor resistance	$R_r = 2.12\ \Omega$
Stator leakage inductance	$L_s = 0.022$ H
Rotor leakage inductance	$L_r = 0.006$ H
Resultant magnetizing	$L_m = 0.3672$H
Moment of inertia	$J = 0.0662$ kg.m^2
Viscous friction coefficient	$K_f = 0.001$ kg.m^2/s

6. Simulations results

The efficiency and robustness of the proposed FTC compared to the BSC in post-fault operation are shown through simulation results using MATLAB/Simulink environment. The reference speed is set at 200 rd/s, a nominal load torque is applied at t=1s then a faults effect is introduced at t=1.5 sec, throughout the simulation, the value of the reference flux is maintained at 1 Wb thanks to a weakening block. The nominal electrical and mechanical parameters of the machine studied in this paper are given in Table 2. The simulations presented in Fig. 5 show DSIM responses in healthy

and defective mode. The results showed the superior performance of the proposed FTC.

During the un-faulty mode, the speed follows its reference value with a negligible overshoot and without oscillations, BSC has a fast dynamic response and a short transient regime, the load torque is very well compensated by the electromagnetic torque (before t=1.5s) but it is clear that after the fault occurrence, an abnormal behavior of the DSIM is observed with the BSC accompanied by a closed-loop performance degradation; velocity oscillations are visible in Fig. 5 (a) and (b). The stator phase current is not sinusoidal, the distortion of the signal is caused by the faults effect, the oscillations on this physical quantity are clearly indicated on Fig. 5 (c) and (d), its amplitude can reach up to ±14 A greater than the nominal value. The flux trajectory is presented in Fig. 5 (e); BSC provide weak ripples after the appearance of faults. High ripples in the electromagnetic torque can be seen in Fig. 5 (f), where the maximum positive ripple reaches +60N.m and the maximum negative ripple reaches -42 N.m. Regarding the proposed FTC, oscillations in rotor speed are completely eliminated, the proposed FTC guarantees a better speed response with accurate reference tracking and also provides better stability with the smallest
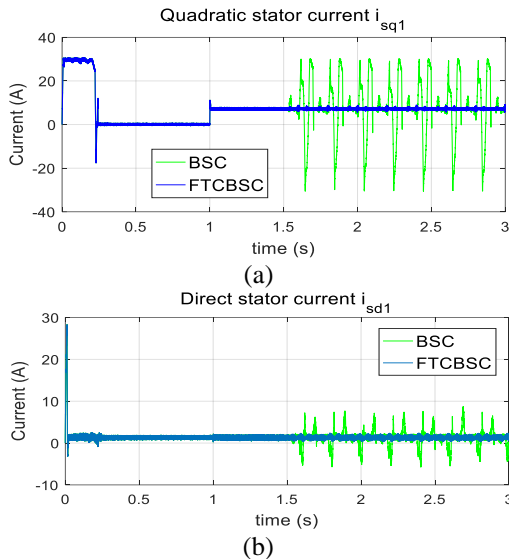
598

Figure. 6 Currents i_{sd1} and i_{sq1} in case of three faults (BF, ITSC and BRB) affect the DSIM at time t=1.5 s using BSC and proposed FTC: (a) quadratic stator current i and (b) direct stator current i
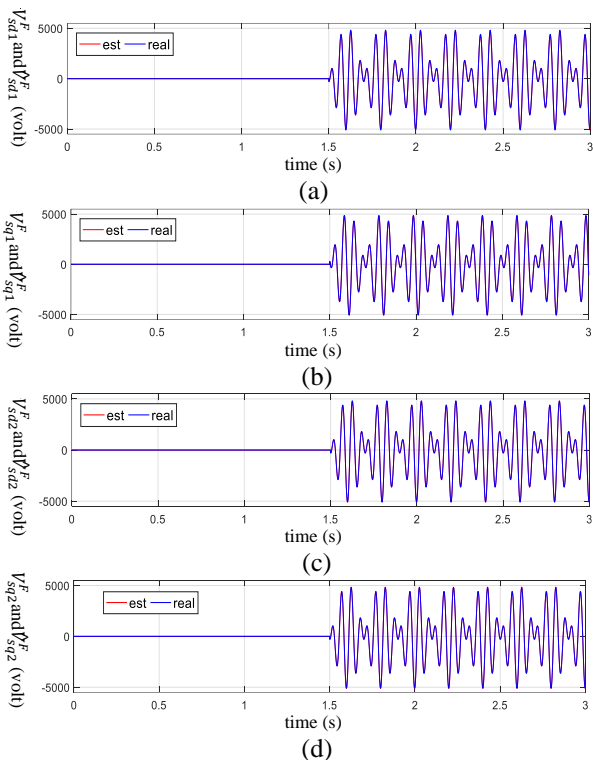

Figure. 7 Real and estimated faults in case of three faults (BF, ITSC and BRB) affect the DSIM at time t=1.5 s when using the proposed FTC: (a) V_{sd1}^F and $\hat{V}_{sd1}^F$ (b) V_{sq1}^F and $\hat{V}_{sq1}^F$ (c) V_{sd2}^F and $\hat{V}_{sd2}^F$ (d) V_{sq2}^F and $\hat{V}_{sq2}^F$

average static error. The tracking performance of the stator

Currentis excellent, the current signal is sinusoidal. Fig. 5 (e) proves that the proposed FTC is able to correctly lead the flux to its desired reference (1Wb) even under faults. No ripple in the electromagnetic torque signal during faulty

Table 4. RMSE values for the proposed control, and proposed control in [18-20]

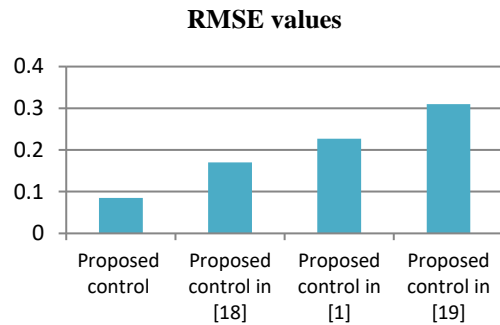| Controller Types	RMSE values
Proposed control	**0.0851**
Proposed control in [18]	0.1702
Proposed control in [1]	0.2267
Proposed control in [19]	0.3102

Figure. 8 RMSE histogram of the proposed control, and proposed control in [18-20]

operation as shown in Fig. 5 (f). Finally, simulation results show that defects do not affect the performance of the proposed FTC, even in the presence of load torque, while BSC fails to handle the unbalanced machine correctly.

Fig. 6 presents the direct and quadratic current components that reflect the temporal evolution of rotor flux and electromagnetic torque, respectively.

The next figure shows the performance of the Thau observer in estimating unknown additive faults V_{sd1}^F, V_{sq1}^F, V_{sd2}^F and V_{sq2}^F. It is clear that the nonlinear observer can accurately detect and estimate uncertainties.

7. Performance comparison

For quantitative comparison between four previous control methods, root-mean-square error (RMSE) is used as the comparison criteria. Table 4 and Fig. 8 shows the RMSE values of the numerical simulation results in faulty operation using the proposed control approaches proposed in [18-20] and the proposed control in this paper. It is observed that the proposed control method offers the smallest values control of RMSE, whereas the proposed control in [19] present the largest values of RMSE. It can be seen that the system performances are better, when using the proposed the proposed control as compared to the proposed control approaches proposed in [18-20].

8. Conclusions

This paper highlights the importance of active

fault tolerant control for double star induction machine. This method is appropriate for a large faults range of the DSIM. After making a DSIM fault model, a nonlinear Thau observer with an adaptive fault estimation law is designed to provide precise state estimates and reconfigure the control system to preserve the machine performances even under load torque. After the occurrence of faults, the proposed FTC is activated by introducing the fault estimation information into the control law where the global stability of the post-fault system is proved using Lyapunov stability theorem. Finally, the effectiveness and robustness of the proposed FTC have been illustrated in simulation by MATLAB/Simulink. The obtained results show that the proposed fault-tolerant approach has excellent tracking performances and strong fault-tolerance for different faults. The proposed FTC could be a realistic solution and a powerful alternative to existing FTC methods. Moreover, computer numerical simulation based on deferent faults (broken rotor bars, end-rings) scenarios in double star induction machine show the effectiveness of the proposed approach.

References

[1] N. Layadi, A. Djerioui, S. Zeghlache, H. Mekki, A. Houari, J. Gong, and F. Berrabah, "Fault-Tolerant Control Based on Sliding Mode Controller for Double-Star Induction Machine", *Arabian Journal for Science and Engineering*, Vol. 45, pp 1615–1627, 2020.

[2] L. Ana, M. Herrera, E. R. F. Alvarez, L. M. L. Carrillo, R. I. M. Chavez, M. L. Ramirez, and E. C. Yepez, "Multiple Fault Detection in Induction Motors through Homogeneity and Kurtosis Computation", *Journal of Energies*, Vol. 15, p. 1541, 2022.

[3] M. J. Guarneros, C. M. Perez, and J. R. Magdaleno, "Diagnostic of Combined Mechanical and electrical faults in ASD-powered Induction Motor using MODWT and a Lightweight 1D CNN", *IEEE Transactions on Industrial Information*, 2021, doi: 10.1109/TII.3120975.

[4] M. E. E. DineAtta, D. K. Ibrahim, M. Gilany, and A. F. Zobaa, "Incipient Broken Bar Faults at Various Load and Inertia Conditions", *Journal of Sensors*, Vol. 22, No. 365, 2022.

[5] S. HwanIm and B. G. Gu, "Study of Induction Motor Inter-Turn Fault Part II: Online Model-Based Fault Diagnosis Method", *Journal of Energies*, Vol. 15, No. 977, 2022

[6] Y. Wang, N. Xu, Y. Liu, and X. Zhao, "Adaptive fault-tolerant control for switched nonlinear systems based on command filter technique", *Applied Mathematics and Computation*, Vol. 392, 2021.

[7] M. Manohar and S. Das, "Current sensor fault-tolerant control for direct torque control of induction motor drive using flux-linkage observer", *IEEE Transactions on Industrial Informatics*, Vol. 13, No. 6, pp. 2824-2833, 2017.

[8] Y. Azzoug, R. Pusca, M. Sahraoui, A. Ammar, T. Ameid, R. Romary, and A. Cardoso, "An Active Fault-Tolerant Control Strategy for Current Sensors Failure for Induction Motor Drives Using a Single Observer for Currents Estimation and Axes Transformation", *European Journal of Electrical Engineering*, Vol. 23, No. 6, 2021.

[9] L. Yi, T. Sun, W. Yu, X. Xu, G. Zhang, and G. Jiang, "Induction motor fault detection by a new sliding mode observer based on backstepping", *Journal of Ambient Intelligence and Humanized Computing*, 2022, doi: 10.1007/s12652-022-03755-7.

[10] R. Tabasiana, M. Ghanbaria, A. Esmaeli, and M. Jannati, "A novel speed control strategy for 3-phase induction motor drives with star-connected under single-phase open-circuit fault using modified RFOC strategy", doi.org/10.1016, 2021.

[11] J. Kellner, S. Kaščák, and Ž. Ferková, "Investigation of the properties of a five-phase induction motor in the introduction of new fault-tolerant control", *Applied Sciences*, Vol. 12, No. 2249, 2022.

[12] A. Gholipour, M. Ghanbari, E. Alibeiki, and M. Jannati, "Speed sensorless fault-tolerant control of induction motor drives against current sensor fault", *Electrical Engineering*, Vol. 103, pp. 1493-1513, 2021.

[13] E. Elbouchikhi, V. Choqueuse, F. Auger, and M. Benbouzid, "Motor Current Signal Analysis Based on a Matched Subspace Detector", *IEEE Transactions on Instrumentation and Measurement*, Vol. 66, No. 12, pp. 3260-3270, 2017.

[14] J. Guo, J. Qi, and C. Wu, "Robust fault diagnosis and fault-tolerant control for non linearquadrotor unmanned aerial vehicle system with unknwn actuator faults", *International Journal of Advanced Robotic Systems*, 2021, doi: 10.1177/17298814211002734.

[15] M. Mansouri, M. Bey, S. Hassaine, M. Larbi, T. Allaoui, and M. Denai, "Genetic algorithm optimized robust nonlinear observer for a wind

turbine system based on permanent magnet synchronous generator", *Elsevier*, 2022, doi. 10.1016/j.isatra.2022.02.004.

[16] S. Dey, P. Pisu, and B. Ayalew, "A Comparative Study of Three Fault Diagnosis Schemes for Wind Turbines", *IEEE Trans. Contr. Sys. Techn*, Vol. 23, No. 5, pp. 1853-1868, 2015.

[17] S. Zeghlache, T. Benslimane, and A. Bouguerra, "Active fault tolerant control based on interval type-2 fuzzy sliding mode controller and non linear adaptive observer for 3-DOF laboratory helicopter", *ISA Transactions*, Vol. 71, pp. 280-303, 2017.

[18] O. Aichetoune, "Robust Nonlinear Controller of the Speed for Double Star Induction Machine in the Presence of a Sensor Fault", *International Journal of Intelligent Engineering and Systems*, Vol. 13, No. 3, 2020, doi: 10.22266/ijies.0630.12.

[19] A. Guezmil, H. Berriri, A. Sakly, and M. F. Mimouni, "Sliding Mode-Based Active Fault-Tolerant Control for Induction Machine", *Journal of Electrical Engineering*, Vol. 45, pp. 1447-1455, 2020.